Thin-Walled Structures 180 (2022) 109959

Contents lists available at ScienceDirect

Thin-Walled Structures

journal homepage: www.elsevier.com/locate/tws

Full length article

Web-post buckling prediction resistance of steel beams with elliptically-based web openings using Artificial Neural Networks (ANN)

Rabee Shamass [a,*], Felipe Piana Vendramell Ferreira [b], Vireen Limbachiya [a], Luis Fernando Pinho Santos [a], Konstantinos Daniel Tsavdaridis [c]

[a] London South Bank University, School of Built Environment and Architecture, London, UK
[b] Federal University of Uberlândia, Faculty of Civil Engineering – Campus Santa Mônica, Uberlândia, Minas Gerais, Brazil
[c] Department of Engineering, School of Science and Technology, City, University of London, Northampton Square, EC1V 0HB, London, UK

ARTICLE INFO

Keywords:
Artificial Neural Network
Classifications
Machine learning
Perforated beams
Elliptically-based web openings
Web-post buckling

ABSTRACT

This paper aims to propose an Artificial Neural Network (ANN) model that predicts accurately web-post buckling resistance and failure mode of steel beams with elliptically-based openings. A total of 4,344 and 5,400 geometrical models, were developed by finite element method (FEM) and used to train, validate and test the ANN model for the web-post resistance and failure mode classification, respectively. It was concluded that five neurons model were sufficient to predict the web-post buckling resistance and the failure mode with high level of accuracy. The height and the web thickness of the beams had positive impact of the capacity while the web openings height, width and radius of the elliptically-based web opening were the geometric parameters that had negative impact of the capacity. At last, an ANN-based formula was proposed and compared with previous analytical model for web-post buckling resistance of elliptically-based openings, which considered the web-post as a truss model. The ANN-based formula showed high accuracy, since the Regression (R^2), Root Mean Square Error (RMSE), Mean Absolute Error (MAE), Average (FEM/Predicted), Standard Deviation and Variation were 0.9989, 26.03 kN, 15.0 kN, 1.00, 4% and 0.12%, respectively. Consequently, the ANN-based formula for web-post buckling resistance of steel beams with elliptically-based openings can be safely adopted for design purposes.

1. Introduction

The use of steel beams with periodical web openings has the advantage of reducing the self-weight and deflections while increasing spans reducing the structural depth per floor by integrating electric and hydraulic services. Also, the web openings favor the flow of air in closed environments, such as parking. The web openings can have different geometries. Steel beams with hexagonal, circular and sinusoidal web openings are known as castellated, cellular and Angelinas™ [1], respectively. The present study focuses on steel beams with novel elliptical web openings, whose patent, GB 2492176 was developed by Tsavdaridis and D'Mello [2].

Although steel beams with periodical web openings possess a number advantages, they are more susceptible to instability phenomena, such as web and flange local, web distortion, lateral–torsional and web-post buckling modes, or even the interaction between them [3–9]. Web-post buckling occurs for steel beams with web openings which have a reduced web-post width [10]. This buckling mode is characterized by a lateral displacement with torsion due to horizontal shear which creates a strut-tie model. The geometric parameters that influence the web-post buckling resistance are the opening height, the web-post width and the web thickness [11–14]. The web-post buckling resistance design models for the cellular and castellated beams are found in publications, such as SCI P355 [15] and Steel Design Guide 31 [16]. On the other hand, in relation to Angelinas™ beams, the calculation models are found in the software Angelina/ArcelorMittal [1]. These prediction models are consolidated in the literature.

Regarding the perforated steel beams with elliptically-based web openings, although there are some studies that have highlighted the efficiency of the openings in relation to their structural behavior, i.e., Tsavdaridis and D'Mello [17], Tsavdaridis [18] and Tsavdaridis et al. [19], little investigation has been carried out with respect to web-post buckling resistance prediction models. Tsavdaridis and D'Mello [12] proposed an equation to predict the web-post buckling. The prediction model was developed considering a parametric study by finite element (FE) method. However, the resistance model is only

* Corresponding author.
E-mail addresses: shamassr@lsbu.ac.uk (R. Shamass), fpvferreira@ufu.br (F.P.V. Ferreira), limbachv@lsbu.ac.uk (V. Limbachiya), pinhosl3@lsbu.ac.uk (L.F.P. Santos), konstantinos.tsavdaridis@city.ac.uk (K.D. Tsavdaridis).

https://doi.org/10.1016/j.tws.2022.109959
Received 2 June 2022; Received in revised form 18 July 2022; Accepted 1 August 2022
Available online xxxx

Notation

The following symbols are used in this paper:

b_f	the flange width;
d	the parent section height;
d_g	the total height after castellation process;
d_o	the opening height;
d_t	the tee height;
$f_{cr,w}$	the critical shear stress in the web-post;
h	the distance between flanges geometric centers of the parent section;
H	the distance between flanges geometric centers after castellation process;
k	Coefficient in Eq. (1);
K	Coefficient in Eq. (8);
l_{eff}	the web-post effective length;
R	the opening radius;
s	the web-post width;
t_f	the flange thickness;
t_w	the web thickness;
V	the global shear;
w	the opening width;
λ_0	the reduced slenderness factor;
λ_w	the web-post slenderness factor;
χ	the reduction factor;

applied to a limited range of geometric configurations. Recently, Ferreira et al. [20] proposed a model for predicting the web-post buckling resistance of steel beams with elliptically-based openings. For this task, 4344 geometric configurations were considered in the parametric study. The procedure is an adaptation of the strut-tie model analogy, which takes into account the web-post effective length, and the buckling stress is calculated based on EC3 [21], according to Eqs. (1)–(10).

$$l_{eff} = k\sqrt{\left(\frac{d_o - 2R}{2}\right)^2 + \left(\frac{s}{2} - R\right)^2} \tag{1}$$

$$k = 0.516 - 0.288\left(\frac{H}{d_o}\right) + 0.062\left(\frac{s}{s-w}\right) + 2.384\left(\frac{s}{d_o}\right) - 2.906\left(\frac{w}{d_o}\right) \tag{2}$$

$$\lambda_w = \frac{l_{eff}\sqrt{12}}{t_w} \tag{3}$$

$$f_{cr,w} = \frac{\pi^2 E}{\lambda_w^2} \tag{4}$$

$$\lambda_0 = \sqrt{\frac{f_y}{f_{cr,w}}} \tag{5}$$

$$\phi = 0.5\left[1 + 0.49\left(\lambda_0 - 0.2\right) + {\lambda_0}^2\right] \tag{6}$$

$$\chi = \frac{1}{\phi + \sqrt{\phi^2 - {\lambda_0}^2}} \leq 1.0 \tag{7}$$

$$\sigma_{Rk} = K\chi f_y \tag{8}$$

$$K = -1.318 + 1.790\left(\frac{H}{d_o}\right) + 0.413\left(\frac{s}{s-w}\right) - 1.926\left(\frac{s}{d_o}\right) + 0.937\left(\frac{w}{d_o}\right) - 0.02\left(\frac{d_o}{t_w}\right) + 1.412\lambda_0 \tag{9}$$

$$V_{Rk} = \sigma_{Rk} t_w (s - w) \tag{10}$$

In the recent years, researchers have utilized Machine Learning (ML) methods to study the performance of structures. They are capable of teaching the computer systems on how to make predictions from databases and algorithms, and have the ability to learn and improve themselves [22]. Artificial Neural Networks (ANN) have become the most popular ML method in structural engineering. The architecture of an ANNs consists of interlinked nodes displayed in 3 or more layers (input layer, hidden layers, and output layer). This nodal connectivity allows the ANN to attain complex relations by interpreting patterns between the inputs and outputs.

ANN has been recently employed in many structural engineering applications such as damage detection of structures and capacity prediction and reliability analysis of steel and concrete structural elements. Gholizadeh et al. [23] used a 4-noded, single hidden layer ANN to accurately predict the web-post load carrying capacity of castellated steel beams from a dataset obtained from the numerical analysis of 140 FE models. Sharifi and Tohidi [24] used 21 numerical models to train an ANN model that estimates the elastic buckling capacity of steel girders with rectangular web openings. Two other ANN models were developed to predict the lateral–torsional buckling capacity and the bearing capacity of corroded steel beams with rectangular web openings [25,26]. With a dataset of 99 numerical models of simply supported cellular beams under four-point bending, Sharifi et al. [27] predicted the strength capacity of cellular beams under lateral–torsional buckling. Different training algorithms and ANN architectures were tested to predict this phenomenon in the most efficient manner [28]. Lateral–distortional buckling mode of steel castellated beams was researched by Hosseinpour et al. [29], where an ANN showed superior predictions of the ultimate moment capacity than the ones shown in current design codes. Nguyen et al. [30] explored an optimal ANN architecture to predict the bearing capacity of castellated steel beams with 150 experimental results. A single-layer, single-neuron neural network was sufficient to predict the load-carrying capacity of these beams, showing that a small ANN architecture can be used to better understand structural behavior. Abambres et al. [31] developed an ANN model for simply supported beams under uniform loads using a numerical database of 3645 numerical models. The proposed method could accurately predict the elastic buckling load of such structural elements. Limbachiya and Shamass [13] developed an ANN model that predicted the web-post buckling resistance of cellular beams from experimental and numerical results. The input parameters and the number of neurons in the hidden layer were varied to establish an efficient architecture. Finally, Ferreira et al. [3] used a numerical dataset of 768 beams to develop an ANN to generate a practical design equation that can accurately describe the lateral–torsional buckling of slender steel cellular beams. The method proved efficient at assessing the lateral–torsional buckling resistance of cellular beams even when this failure mode is combined with web-post buckling or web-distortional buckling modes. Finally, in Vitaliy and Tsavdaridis [32], ML for predicting the elastic buckling and ultimate loads of steel cellular beams were examined and the accuracy of the ultimate load predictions by the ML models exceeded the accuracy provided by the existing design provisions for steel cellular beams published in SCI P355 [15] and Steel Design Guide 31 [16].

Overall, these studies demonstrated that ANN can accurately predict experimental and numerical results of web-post buckling. It is noted that the ANN formula accurately predicts the capacity of perforated steel beams subjected to various loading conditions that fail in different failure modes such as web-post buckling and lateral torsional buckling or the combination of these modes. However, there is currently no research that establishes a comprehensive and practical design model tool, processing large amount of data and using machine learning to predict the web-post buckling capacity of steel beams employing this pioneered patented elliptically-based web openings, which is the main objective of this study. Although Tsavdaridis and D'Mello [33] and Ferreira et al. [20] proposed theoretical models to predict the web-post buckling of steel beams with elliptically-based openings based on the EC3, the current research paper proposes a different method,

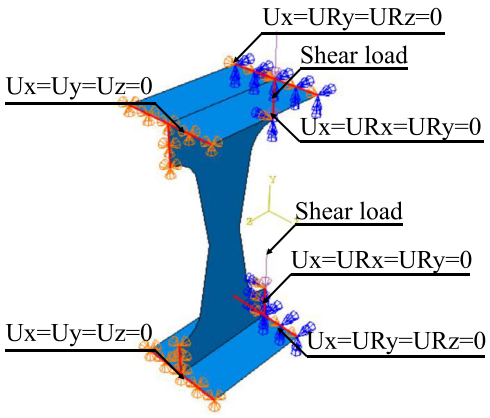

Fig. 1. Boundary conditions.

which is more accurate, reliable and expandable to predict the strength and failure mode of elliptically-based openings beam using machine learning. The study makes use of the dataset provided in Ferreira et al. [20] to train and test the ANN. By using a dataset of 4344 data points, the ANN presented in this paper can predict the web-post buckling capacity under a vast range of geometrical variables, increasing its practical application for structural design.

2. Finite element method: validation and parametric studies

Ferreira et al. [20] previously developed an FE model using the ABAQUS [34] software for both full and single web-post models. The FE models were validated against the tests results conducted by Tsavdaridis and D'Mello [12] and were shown to be capable of providing a good prediction of the behavior of steel beams with perforated web openings in terms of vertical shear resistance and failure modes. In brief, the validation study was carried out in software ABAQUS, considering only web-post models of steel beams with elliptically-based web openings. The modeling of the web-post models allows the identification of failure mechanisms in an isolated way, such as web-post buckling [11,13,14,35–37].

For the validation study, the FE model is processed using ABAQUS software in two steps: buckling and post-buckling analyses [3,4,6,8,14,38–45]. The geometrically and materially nonlinear analysis with imperfections (GMNIA) has been used in the post-buckling analysis. A1, A2, B1, B2 and B3 tests carried out by Tsavdaridis and D'Mello [12] are considered. A multilinear material behavior is used to modeling stress–strain relationship of steel, according to the methodology employed in Shamass and Guarracino [40]. The Young's modulus and Poisson's coefficient are taken equal to 200 GPa and 0.3, respectively. The initial geometric imperfection considered is $d_g/500$. This factor was also used by Panedpojaman et al. [14], since the estimation of physical and geometric imperfections on steel beams with periodical perforated web openings is complex due to the manufacturing castellation process. Mesh convergence study was conducted, and it was found that an element size of 10 mm for all studied cellular beams was sufficient to provide accurate FE results [8,45]. S4R shell element was used which has six degrees of freedom — three rotations and three translations and provides accurate results with less computational effort. The boundary conditions of the web-post models are shown in Fig. 1.

The results of the validation study are presented in Table 1, considering the web-post models. It can be observed that the percental differences between FE and the test shear loads vary between 9.4% to −8.8% with an average of −0.14% and coefficient of variation of 0.14%. Hence, the proposed web-post model is reasonably accurate and used for further parametric studies to predict the shear load capacity of the web-post.

Table 1
Web-post models validation results.

Test	V_{Test} (kN)	V_{FE} (kN)	Failure	$(V_{FE}/V_{Test}-1)$ %
A1	144.4	157.0	WPB	8.8%
A2	149.0	159.0	WPB	6.7%
B1	127.5	121.0	WPB	−5.1%
B2	201.2	200.5	WPB	−0.3%
B3	207.5	188.0	WPB	−9.4%
			S.D.	6.93%
			Var.	0.48%

Regarding the parametric study, twelve UB sections are considered (178 × 102 × 19, 305 × 102 × 25, 305 × 102 × 33, 305 × 127 × 48, 457 × 152 × 52, 457 × 191 × 133, 533 × 210 × 122, 533 × 312 × 272, 686 × 254 × 170, 838 × 292 × 176, 914 × 305 × 201 and 1016 × 305 × 487). For each section, the geometric parameters of the steel beams with elliptically-based web openings are varied (Fig. 2), considering the ratios H/d, d_o/H, R/d_o and w/d_o. These parameter variations are in accordance with the castellation process, as shown in GB 2492176 [2]. Python scripting is used to carry out the parametric study and post-process the results. Further details about the parametric study and Python script were published in Ferreira et al. [19].

3. Development of the Artificial Neural Network (ANN)

5400 numerical models were generated for this parametric study. The failure mode governed either by web-post buckling (WPB) or Vierendeel mechanism (VM) was defined in each model. The web-post buckling resistance, as the vertical shear resistance of the web-post, is obtained from the FE models. Artificial Neural Networks (ANN) and 4344 models are used herein to predict the web-post buckling load and 5400 models are used to classify the failure mode (WPB or VM). The development of a robust ANN model is described below.

3.1. Neural network architecture

An ANN consists of three basic layers: an input layer, hidden layer, and an output layer. The hidden layer is determined by a set number of neurons and provides a connection between each input parameter and the single output parameter. There is a weighted connection between each input parameter and neuron in the hidden layer, as well as a constant bias value between input parameter and neurons. The hidden layer is then connected to the output layer. In the output layer, every connection from the hidden layer is weighted with a value, a transfer function, and a constant bias value. To review predicted values, as the input values are normalized, the output value will have to be denormalized. Thereafter, the error between the predicted and target values can be calculated to assess the accuracy of the model.

Several parameters are needed to derive the ANN model, including the input parameters, number of neurons in the hidden layer, activation function, as well as the output parameter. The input parameters used in this study were the opening height (d_o), the distance between flanges geometric centers after castellation process (H), the opening radius (R), the web thickness (t_w) and the opening width (w). The number of neurons in the hidden layer has an impact on the accuracy of the ANN model. By modeling several networks with a different number of neurons and thereafter comparing their results, the optimal number of neurons in the hidden layer can be determined. In this paper, the ANN network was modeled with 3, 4, 5, 6, 7, 8 and 9 neurons in the hidden layer. Fig. 3a illustrates an example of an ANN structure consisting of 5 input parameters, 3 neurons in the hidden layer, and 1 output parameter. Regarding the failure model classifications, a two-layer (one-hidden layer and output layer) feed-forward network is used. The input features H, t_w, d_o, w and R are parameters governing the failure of perforated beams with elliptically-based web openings beams, while the output variables are two failure modes: WPB (class 1), and

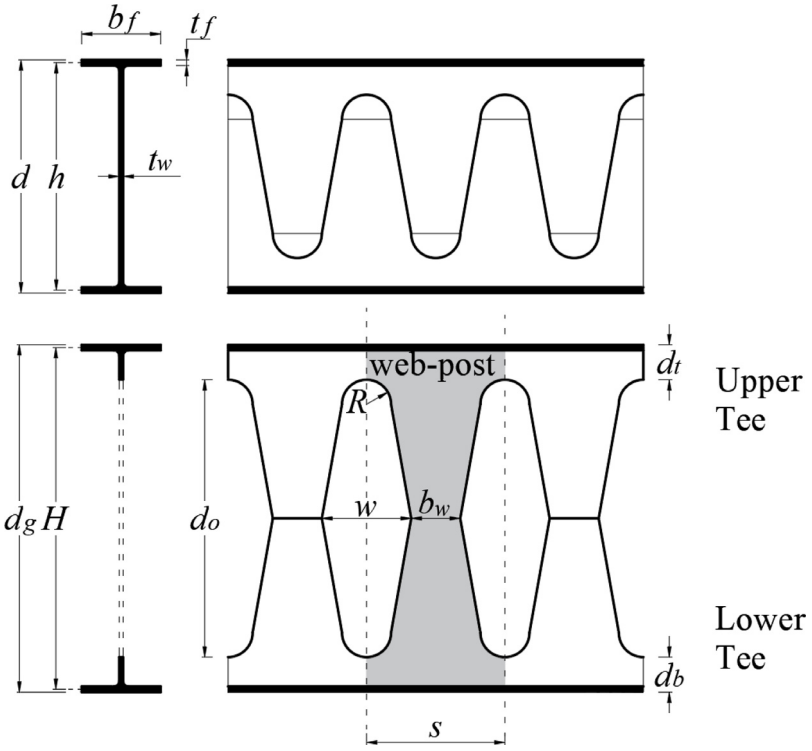

Fig. 2. Geometric parameters of steel beams with elliptical web openings.

VM (class 2). A sensitivity analysis was conducted, for which different ANN models with different number of neurons were considered and the hidden layer with 5 neurons is sufficient to accurately classify the mode of failure. The performance of ANN model was assessed in terms of the cross-entropy error with respect to the number of epochs. Fig. 3b illustrates the ANN framework for the failure mode.

The network architecture described in this paper consists of a Multi-Layer Perceptron Network (MLPN). Two-layer feedforward neural network available in MATLAB's neural network toolbox [46] was employed. Back-Propagation of Multilayer Feedforward ANN adjusts the weights and bias values to minimize the errors. Furthermore, the final weights and bias values between different layers can be used to calculate the influence of input parameters on the outcome parameters.

3.2. Input and output normalization

To improve the learning speed, performance, accuracy, and stability of the training process, normalization for input variables across all data patterns should be adopted [47]. Input parameters were normalized using Eq. (11) [48], where X^{act} is the actual value of the input/output, X_{norm} is the normalized value, X_{min} and X_{max} are the minimum and maximum values of the input/output parameters, respectively (Table 2). Y_{min} is the minimum value for each row of X (default is –1) and Y_{max} is the maximum value for each row of X (default is + 1). To denormalize the output parameters, X^{act} is made to be the subject of the equation, with X^{norm} being the predicted value from the ANN model.

$$X^{norm} = \frac{(Y_{max} - Y_{min})(X^{act} - X_{min})}{(X_{max} - X_{min})} + Y_{min} \tag{11}$$

3.3. Learning (training) algorithm and transfer function

The Levenberg–Marquardt back propagation training algorithm is used in this study because it is fast, has consistent convergence, and can be used to train small and medium-sized problems. A total of 4344 data sets were used in the ANN model. To avoid overfitting the ANN model and providing the most accurate predictions, for both the model prediction and classification, the data points are randomly separated into three sets: training, validation, and testing, with 3040 (70% of data), 652 (15%), and 652 (15%) sets of data in each set respectively. A combination of which 70% of data was used for training, 15% was used for validation and testing led to the best prediction and classification accuracy with ANN models. Therefore, the ANN model is based on this combination. The training set is used to compute the gradient and update the weights and biases, the validation data set is used to perform cross validation so that the network's performance can be generalized and the test data set is used to check the ANN accuracy after the optimum network parameters have been defined. Eqs. (12)–(13) show the hyperbolic tangent transfer function that is required to determine the normalized output value based on the inputs provided [47].

Table 2
Parameters used to normalize input and target values.

Input/Target Parameter	X_{min}	X_{max}	Y_{min}	Y_{max}
H (mm)	213.36	1658.1	–1	1
t_w (mm)	4.8	30	–1	1
d_o (mm)	138.68	1492.3	–1	1
w (mm)	34.67	916.09	–1	1
R (mm)	13.87	422.81	–1	1
V (kN)	39.44	4301.4	–1	1

$$O_s = B_1^s + \sum_{k=1}^{r}\left(w_{k,l}^{ho}\frac{2}{1+e^{-2H_k}} - 1\right) \tag{12}$$

$$H_k = B_2^k + \sum_{j=1}^{q} w_{j,k}^{ih} \cdot I_j \tag{13}$$

where, O_s represents the normalized output value, q is the number of input parameters; r is the number of hidden neurons; s is the number

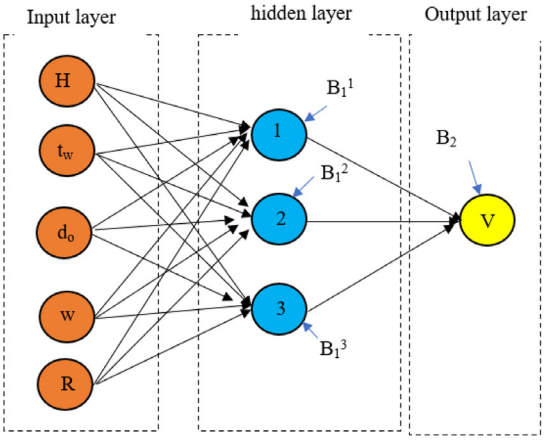

(a) ANN Model with 3 neurons in the hidden layer

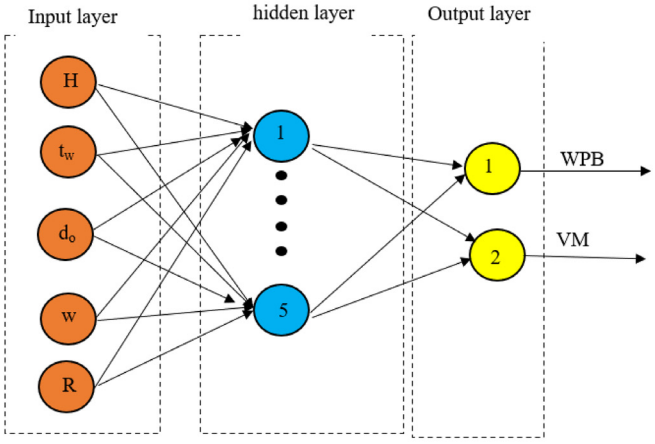

(b) Schematic of the proposed ANN framework for the failure model

Fig. 3. ANN proposed model.

of output parameters; B_1^s and B_2^k are the biases of sth output neuron and kth hidden neuron (H_k), respectively; $w_{j,k}^{ih}$ is the weights of the connection between I_j and H_k; $w_{k,l}^{oh}$ are the weights of the connection between H_k and O_s.

3.4. Assessing the accuracy of neural network

To review the accuracy of the ANN model, it is important to compare the target values to the predicted values. Therefore, the Correlation coefficient (R), Root Mean Square Error ($RMSE$) and Mean Absolute Error (MAE) were calculated using Eqs. (14)–(16), where t_i and O_i are the actual and predicted WPB capacities, N is the total number of data points in each set of data. $\overline{O}$ and $\bar{t}$ are the average of the predicted and actual vertical shear resistance.

$$R = \frac{\sum_{i=1}^{N}\left(O_i - \overline{O}_i\right)\left(t_i - \bar{t}_i\right)}{\sqrt{\sum_{i=1}^{N}\left(O_i - \overline{O}_i\right)^2 \sum_{i=1}^{N}\left(t_i - \bar{t}_i\right)^2}} \tag{14}$$

$$RMSE = \sqrt{\frac{\sum_{i=1}^{N}\left(O_i - t_i\right)^2}{N}} \tag{15}$$

$$MAE = \frac{1}{N}\sum_{i=1}^{N}\left|O_i - t_i\right| \tag{16}$$

3.5. Quantifying input variable contributions in ANN

In this section, the methodology for evaluating the contribution of each variable to web-post buckling resistance of steel beams with elliptically-based web openings is presented.

3.5.1. Connection weight approach

In addition to assessing the accuracy of the model through a comparison between the predicted ANN values and the actual values, it is important to understand the effect of the input parameter on the predicted output. The connection weight approach proposed by Olden and Jackson [49], used in previous studies [3,13], calculates the impact of an input parameter. A positive impact will determine that an increase in the input parameter will increase the value of the output parameter and vice versa for a negative impact value. The impact of each input parameter on the output can be determined using Eq. (17) [38] where, X represents the input parameter, Y is the weighted connection between the input parameter and hidden layer and "*Hidden*" is the weighted connection between the hidden layer and output parameter.

$$Input_X = \sum_{Y=A}^{E} Hidden_{XY} \tag{17}$$

3.5.2. Garson's algorithm

Garson [50] proposed a method to define the relative importance of each input parameter in the neural network. It has been used by many researchers [51–53]. It is worth mentioning that the Garson's

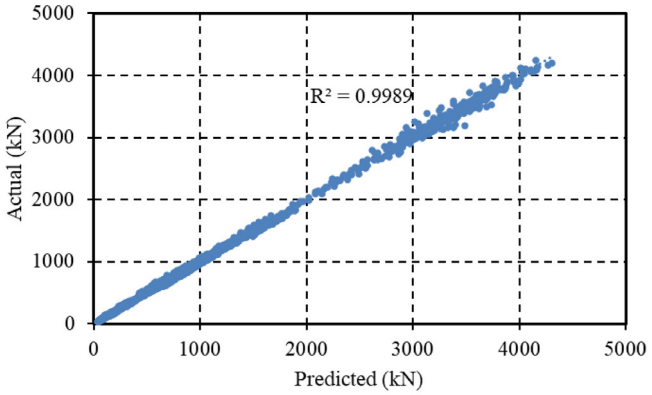

(a) 5-Neuron

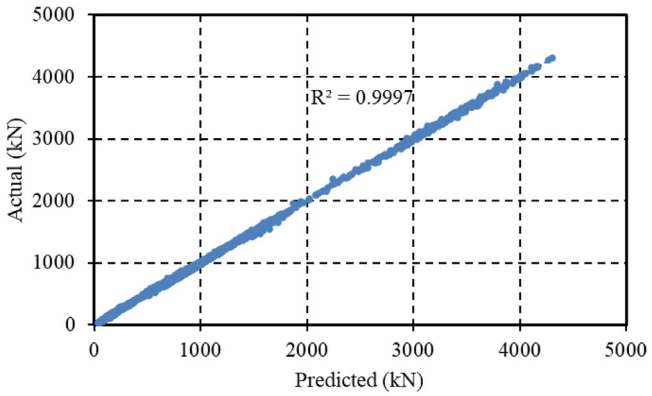

(b) 9-Neuron

Fig. 4. Actual vs. predicted.

algorithm calculates the input variable contribution using the absolute values of the connection weights, therefore, this method does not provide the direction of the relationship between the input and output variables [54].

The relative importance of the jth input parameter on the output is presented in Eq. (18). N_i and N_h are the numbers of neurons in the input and hidden layers, respectively; w is connection weights; the subscripts k, m, and n refer to input, hidden, and output neurons, respectively, and the superscripts i, h, and o refer to input, hidden, and output layers, respectively.

$$I_j = \frac{\sum_{m=1}^{m=Nh}\left(\frac{w_{jm}^{ih}}{\sum_{k=1}^{Ni} w_{km}^{ih}} w_{mn}^{ho}\right)}{\sum_{k=1}^{k=Ni}\left[\sum_{m=1}^{m=Nh}\left(\frac{w_{km}^{ih}}{\sum_{k=1}^{Ni} w_{km}^{ih}} w_{mn}^{ho}\right)\right]} \tag{18}$$

4. Results and discussion

Table 3 provides the R^2 and MSE values for the data sets during the training, validation, and testing stage of the ANN and the R^2, MAE and RMSE for all the data. The results show a clear correlation between the accuracy of the model and the set number of neurons in the hidden layer. As the number of neurons increase, so does the accuracy of the model. However, the increases in neurons also leads to a more complicated formula and potentially produces models that are overtraining. This in terms of real-life application is a disadvantage due to the complexity of the equations that are produced. However, when comparing the 5-neuron model to the 9-neuron model with all the data, the R^2, MAE and RMSE was 0.9989, 15, 26.03, and 0.9997, 8.71, 12.52, respectively. This shows that although the accuracy has increased, a 5-neuron model is still incredibly accurate and has the potential to be used in predicting the output.

Fig. 4a and b provide the predicted against actual results for the 5 and 9 neurons model, respectively. Although the accuracy is slightly greater in the 9-neuron model, the accuracy of the 5-neuron model is still extremely high. Therefore, based on the data in Table 3, it can be assumed that a 5-neuron model will provide a more practical solution for industrial applications yet it will provide a high level of predictive accuracy.

To further assess the validity of the models, the weighted values between the input-hidden and hidden-output layers were used to assess the impact of the input parameters using the connection weight approach and Garsons algorithm. Fig. 5 provides the results of the connection weight approach and depicts the impact of each input parameter on the output parameter for all models that were developed. Results show consistency in the parameters that have the largest impact as well as those parameters that have a positive or negative impact. Results show that as the height of the beam (H) and the web thickness (t_w) increase, the value of the output parameter increases (i.e., the shear resistance/capacity), where H has a greater impact on the capacity than t_w. The analysis also shows that as the opening height (d_o), opening radius (R), or opening width (w) increase, the value of the output parameter decreases. The parameter that has the greatest negative impact on capacity is the opening height, followed by the opening radius and thereafter the opening width. This creates further validity of the ANN prediction as the greater the web thickness, the smaller the web-post slenderness and greater the resistance. Furthermore, increasing the opening height, and opening radius would have a reduction on the height of the tee section, resulting in resistance reduction. Additionally, as the height H increases, the slenderness of the web-post increases as well as the height of the tee sections increases, resulting in an increase in the vertical shear resistance of the web-post. This is valid as the

Table 3
Comparison of statistical values to evaluate the accuracy of the ANN models with different neurons.

Number of neurons	R^2			*MSE*			All data		
	Training	Validation	Testing	Training	Validation	Testing	RMSE	MAE	R^2
3	0.99932	0.99936	0.999	1.89×10^{-4}	1.64×10^{-4}	2.65×10^{-4}	28.89	20.3	0.9986
4	0.99937	0.99933	0.99935	1.74×10^{-4}	1.57×10^{-4}	1.86×10^{-4}	28.11	18.68	0.9987
5	0.99951	0.99931	0.99933	1.33×10^{-4}	2.04×10^{-4}	1.67×10^{-4}	26.03	15.0	0.9989
6	0.99967	0.9997	0.99961	8.66×10^{-5}	9.7×10^{-5}	1.08×10^{-4}	20.37	14.18	0.9993
7	0.99979	0.99973	0.99968	5.89×10^{-5}	6.93×10^{-5}	8.53×10^{-5}	17.1	11.67	0.9995
8	0.99983	0.99983	0.99979	4.58×10^{-5}	5.29×10^{-5}	5.12×10^{-5}	14.72	10.03	0.9996
9	0.99988	0.99988	0.99982	3.26×10^{-5}	3.51×10^{-5}	4.28×10^{-5}	12.52	8.71	0.9997

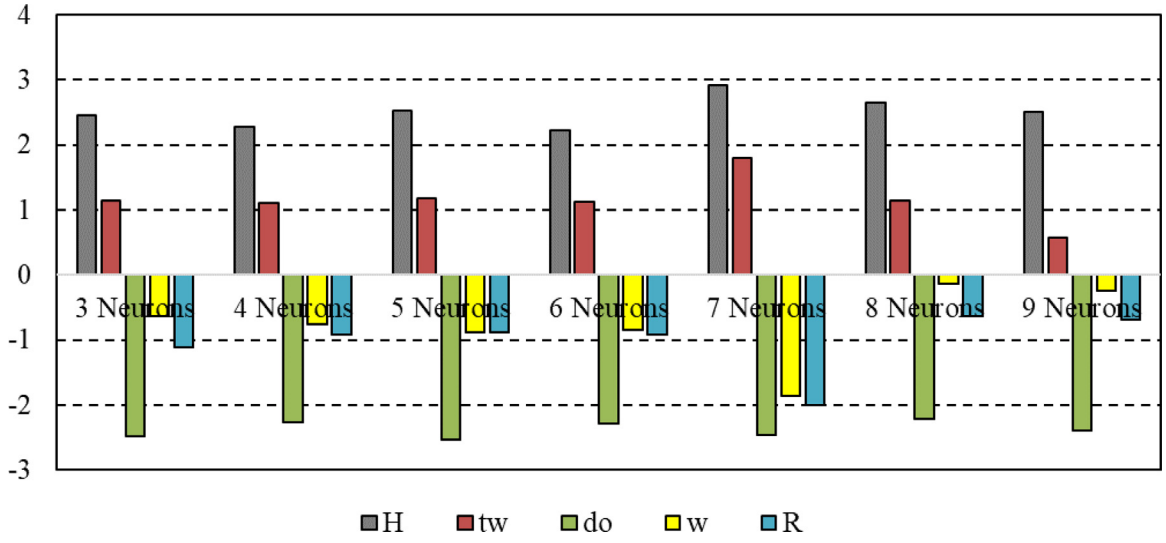

Fig. 5. Impact of input parameters on the resistance.

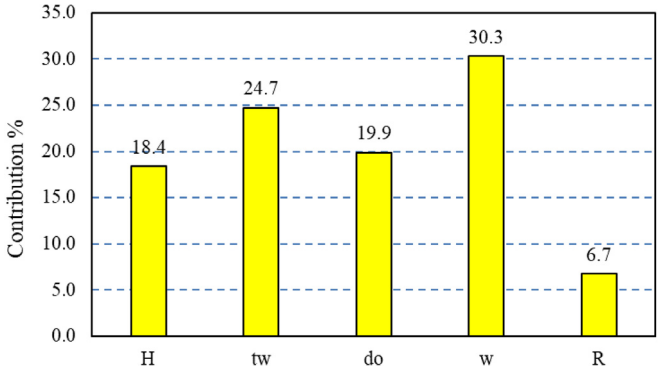

Fig. 6. Contribution (%) of input parameters to the resistance (5 neurons).

geometric ratios (d_o/H, w/d_o and R/d_o) and the web thickness must remain constant.

Fig. 6 illustrates the importance of the five input parameters. The most important input corresponds to highest contribution value calculated using Garson algorithm as explained in Section 3.5.2. It can be observed that the beam height, web thickness as well as web opening height and width of the perforated beams are the significant parameters on the shear resistance, while the opening radius R has less effect on the resistance. Fig. 6 also shows the percentage contribution of each input parameter to the shear resistance. The contribution of the input parameters H, t_w, d_o, w and R is 18.4%, 24.7%, 19.9%, 30.3%, and 6.7%, respectively. In conclusion, as the ANN model with five neurons provides predictions with high level of accuracy and the impact of the inputs on the resistance is as physically expected, it will be used in the following sections.

Fig. 7 represents the performance of the failure classification prediction using ANN. The figure shows the cross-entropy error as a function of epochs. It can be noted that as the epoch increases the cross-entropy error decreases, indicating that the accuracy of the predictions increases. The neural network training was ended when the generalization stopped improving, to prevent overfitting, at which the best validation performance for the ANN classification model is obtained. At this point, indicated by the green circle in Fig. 7, the best validation performance with minimal cross-entropy error is 0.0881 at epoch 57.

To evaluate the performance of the ANN in classification, a confusion matrix was used (Fig. 8). On the confusion matrix, the rows correspond to the predicted class while the columns correspond to

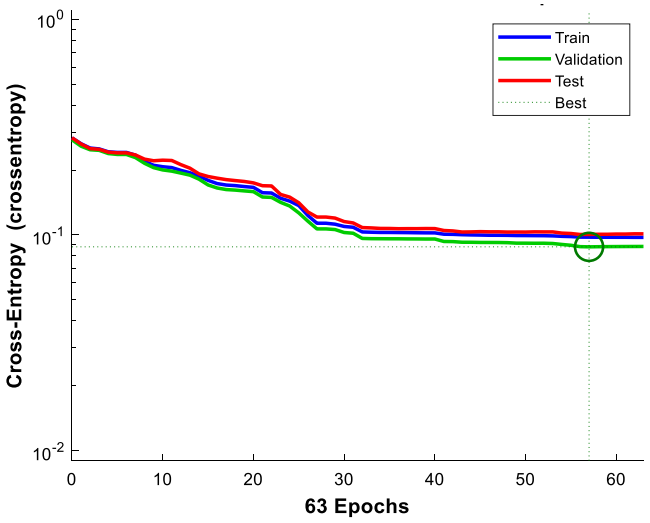

Fig. 7. Performance evaluation of ANN in terms of cross-entropy against number of epochs.

the true/target class [46]. As previously highlighted, classes 1 and 2 represent the WPB and VM failure modes of the beams, respectively. The diagonal cells of the matrix illustrate failure modes that are correctly classified. The off-diagonal cells correspond to incorrectly classified failure mode. The number of the observed failure modes and the percentage of the total number of failure modes are shown in each cell. For example, 4212 failure cases are correctly classified as WPB. This corresponds to 78% of all 5400 data. Similarly, 820 failure cases are correctly classified as VM. This corresponds to 15.2% of all data. The column on the far right of the matrix shows the percentages of correct and incorrect classifications for each predicted failure mode. Out of 4448 WPB failure predictions, 94.7% are correct while 5.3% are wrong. Out of 952 VM failure predictions, 86.1% are correct while 13.9% are wrong.

The row at the bottom of the matrix illustrates the percentages of all cases belonging to each class that are correctly and incorrectly classified. Out of 4344 WBP cases, 97% are correctly predicted as WBP failure and 3% are predicted as VM failure. Out of 1056 VM cases, 77.7% are correctly classified as VM failure and 22.3% are classified as WPB failure. The cell in the bottom right of the matrix indicates the overall classification accuracy. Hence, the overall classification accuracy of the ANN model is 93.2%. This clearly confirms that the ANN algorithm can detect the failure mode (i.e., WPB or VM) of perforated beams with the elliptically-based web openings.

5. ANN-based formula and interactive graphical user interface

An ANN-based formula to predict the normalized shear resistance of the web-post is shown in the Eq. (19). The input parameters, which should fall within X_{max} and X_{min} range as indicated in Table 2, should be normalized using Eq. (11). In order to calculate the normalized shear resistance of the perforated beam with elliptically-based web opening $(V)_n$, the values H_1, $H_2 \ldots$ H_5 should be calculated using Eq. (20) and substituted into Eq. (19). In these equations, $(H)_n$, $(t_w)_n$, $(d_o)_n$, $(w)_n$, and $(R)_n$ represent the normalized values of the inputs H, t_w, do, w and R, respectively, $w_1(i,j)$ are the connection weights between neuron in the hidden layer (i) and input (j), while $w_2(i)$ are the connection weights between the neuron in the hidden layer (i) and the output, as seen in the Table 4. $B_1(i)$ are the bias for each neuron (i) in the hidden layer, and B_2 is the output bias and is equal to 0.077617. To determine the shear resistance (V), denormalization need to be conducted.

$$(V)_n = B_2 + \sum_{i=1}^{n=5} w_2(i)\left(\frac{2}{1+e^{-2Hi}} - 1\right) \tag{19}$$

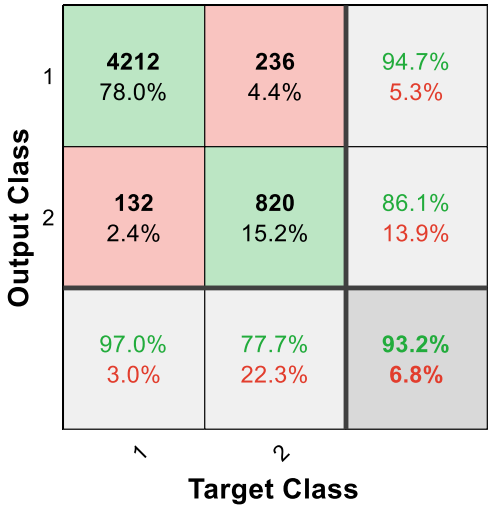

Fig. 8. Confusion matrix based on classification results by ANN.

Table 4
The connection weight and the bias values.

Neuron	$w_1(i,j)$					$w_2(i)$	$B_1(i)$
	H	t_w	d_o	w	R	V	
1	3.8348	1.4794	−3.4851	−5.0850	−2.4212	0.3354	−7.2860
2	0.7013	0.3435	−0.8183	1.0805	−0.2660	−0.8849	0.7064
3	−0.4329	−0.8036	0.5024	0.2778	0.0261	−2.5624	0.9842
4	0.1039	−0.8327	−0.0777	0.9004	0.0056	1.9833	1.1943
5	−0.6187	−0.6568	0.7405	−0.8120	0.2772	−0.8742	−0.6614

$$H_i = B_1(i) + w_1(i,1)(H)_n + w_1(i,2)\left(t_w\right)_n + w_1(i,3)\left(d_o\right)_n + w_1(i,4)(w)_n + w_1(i,5)(R)_n \tag{20}$$

Comparisons between the vertical shear resistance results predicted by FEA with those predicted by Ferreira et al. [20] and ANN formulas are presented in Table 5 and Fig. 9. It can be noted that the ANN overestimates the shear buckling resistance by up to 24.55% while Ferreira et al. [20] analytical model overestimates the shear buckling by up to

Table 5
Statistical comparison between FEA shear buckling results with analytical and ANN predictions.

Analysis	Ferreira et al. [20]	ANN-based formula (Eq. (19))
R^2 (Regression)	0.9871	0.9989
RMSE (Root Mean Square Error) (kN)	91.09	26.03
MAE (Mean Absolute Error) (kN)	46.24	15.0
Minimum relative error	−26.89%	−23.38%
Maximum relative error	28.02%	24.55%
Average (FEM/Predicted)	0.982	1.00
S.D.	7.71%	4%
Var.	0.59%	0.12%

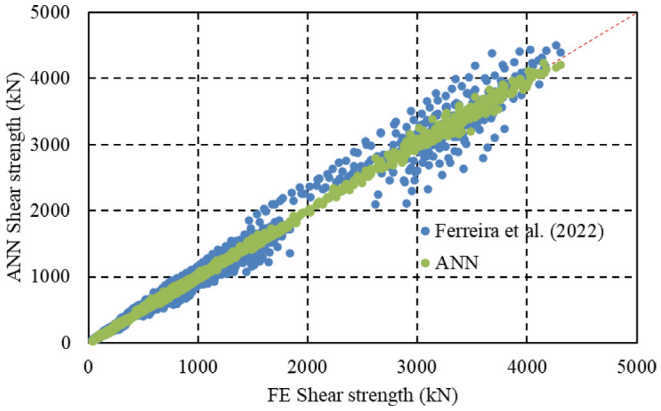

Fig. 9. Comparison of the predicted shear strength with the FE shear strength.

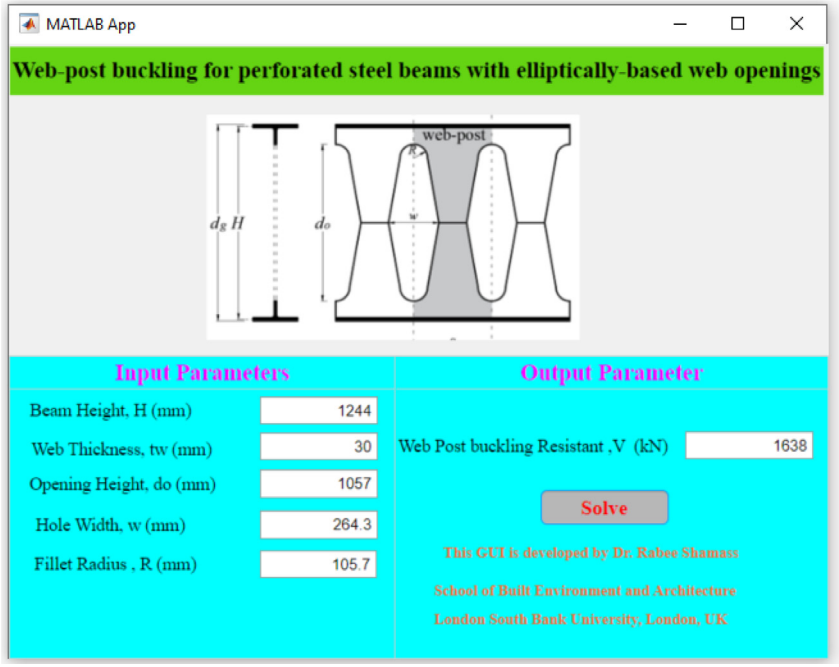

Fig. 10. Interactive graphical user interface.

28.02%. Furthermore, ANN underestimates the shear buckling results by up to 23.38% while Ferreira et al. [20] analytical model underestimates the shear buckling by up to 26.89%. The RMSE and MAE values for the ANN predicted shear resistance are lower than those for Ferreira et al. [20] analytical models and resulting in higher level of accuracy. Based on the regression values, it can be seen that ANN provides the greatest correlation. Fig. 9 shows a graphical representation of ANN and the analytical model together with the FE predictions. Overall, the ANN model tends to provide accurate shear resistance predictions while the analytical models tend to underestimate the predicted web-post shear resistance of perforated beams with elliptically-based web openings.

It can be concluded that the ANN model with five neurons can accurately predict the vertical shear resistance of perforated beams with elliptically-based web openings, hence, the ANN-based formula (Eq. (19)) can be used as a design tool, thus it has been implemented in user graphical interface using MATLAB [46]. Fig. 10 illustrates the main user interface which is simple and easy to use. The user can enter the input parameters of the perforated beam and the web-post buckling resistance is displayed by clicking on Solve button. The

graphical interface is available for users at https://github.com/Rabee-Shamass/ANN

Conclusion

A data-driven machine learning-based computational framework is developed using artificial neural network (ANN) algorithm for predicting the web-post buckling resistance and the failure mode of perforated steel beams with elliptically-based web openings. The proposed framework consists of data generation from FEA, web-post buckling resistance predictions, and failure mode classification. The ANN results were compared with the analytical prediction model. Based on the results, the following conclusions are found:

- The ANN model with five neurons provided web-post buckling resistance predictions with high level of accuracy while the impact of the geometries of the beam on the resistance is as physically expected.
- The proposed ANN-based formula for web-post buckling resistance of steel beams with elliptically-based openings can be safely adopted for design purposes while a design tool has been implemented in user graphical interface using MATLAB and it is free to use.
- ANN algorithm is effective in predicting the failure modes (web-post buckling and Vierendeel mechanism) of perforated beams with the elliptically-based web openings. In this study, the overall accuracy was 93.2%.

CRediT authorship contribution statement

Rabee Shamass: Writing – original draft, Validation, Supervision, Software, Methodology, Investigation, Data curation, Conceptualization. **Felipe Piana Vendramell Ferreira:** Writing – original draft, Validation, Software, Methodology, Investigation, Data curation, Conceptualization. **Vireen Limbachiya:** Writing – original draft, Validation, Software, Methodology, Investigation, Conceptualization. **Luis Fernando Pinho Santos:** Writing – original draft, Validation, Software, Methodology, Investigation, Data curation, Conceptualization. **Konstantinos Daniel Tsavdaridis:** Writing – review & editing, Visualization, Supervision, Software, Methodology, Investigation, Conceptualization.

Declaration of competing interest

The authors declare that they have no known competing financial interests or personal relationships that could have appeared to influence the work reported in this paper.

Data availability

Data will be made available on request.

References

[1] ArcelorMittal, ACB® and Angelina® beams - A new generation of cellular beams, 2018.
[2] K.D. Tsavdaridis, C. D'Mello, Structural beam, 2012, GB 2492176.
[3] F.P.V. Ferreira, R. Shamass, V. Limbachiya, K.D. Tsavdaridis, C.H. Martins, Lateral–torsional buckling resistance prediction model for steel cellular beams generated by Artificial Neural Networks (ANN), Thin-Walled Struct. 170 (2022) 108592, http://dx.doi.org/10.1016/j.tws.2021.108592.
[4] E. Ellobody, Nonlinear analysis of cellular steel beams under combined buckling modes, Thin-Walled Struct. 52 (2012) 66–79, http://dx.doi.org/10.1016/j.tws.2011.12.009.
[5] P. Panedpojaman, W. Sae-Long, T. Chub-Uppakarn, Cellular beam design for resistance to inelastic lateral–torsional buckling, Thin-Walled Struct. 99 (2016) 182–194, http://dx.doi.org/10.1016/j.tws.2015.08.026.
[6] E. Ellobody, Interaction of buckling modes in castellated steel beams, J. Constr. Steel Res. 67 (2011) 814–825, http://dx.doi.org/10.1016/j.jcsr.2010.12.012.
[7] C.M. Weidlich, E.D. Sotelino, D.C.T. Cardoso, An application of the direct strength method to the design of castellated beams subject to flexure, Eng. Struct. 243 (2021) 112646, http://dx.doi.org/10.1016/j.engstruct.2021.112646.
[8] F.P.V. Ferreira, C.H. Martins, LRFD for lateral-torsional buckling resistance of cellular beams, Int. J. Civ. Eng. 18 (2020) 303–323, http://dx.doi.org/10.1007/s40999-019-00474-7.
[9] S.G. Morkhade, L.M. Gupta, Experimental investigation for failure analysis of steel beams with web openings, Steel Compos. Struct. 23 (2017) 647–656, http://dx.doi.org/10.12989/SCS.2017.23.6.647.
[10] D. Kerdal, D.A. Nethercot, Failure modes for castellated beams, J. Constr. Steel Res. 4 (1984) 295–315, http://dx.doi.org/10.1016/0143-974X(84)90004-X.
[11] L.F. Grilo, R.H. Fakury, A.L.R. de Castro e Silva, G. de S. Veríssimo, Design procedure for the web-post buckling of steel cellular beams, J. Constr. Steel Res. 148 (2018) 525–541, http://dx.doi.org/10.1016/j.jcsr.2018.06.020.
[12] K.D. Tsavdaridis, C. D'Mello, Web buckling study of the behaviour and strength of perforated steel beams with different novel web opening shapes, J. Constr. Steel Res. 67 (2011) 1605–1620, http://dx.doi.org/10.1016/j.jcsr.2011.04.004.
[13] V. Limbachiya, R. Shamass, Application of Artificial Neural Networks for web-post shear resistance of cellular steel beams, Thin-Walled Struct. 161 (2021) 107414, http://dx.doi.org/10.1016/j.tws.2020.107414.
[14] P. Panedpojaman, T. Thepchatri, S. Limkatanyu, Novel design equations for shear strength of local web-post buckling in cellular beams, Thin-Walled Struct. 76 (2014) 92–104, http://dx.doi.org/10.1016/j.tws.2013.11.007.
[15] R.M. Lawson, S.J. Hicks, Design of Composite Beams with Large Web Openings. SCI P355, The Steel Construction Institute, 2011.
[16] S.S. Fares, J. Coulson, D.W. Dinehart, AISC Steel Design Guide 31: Castellated and Cellular Beam Design, American Institute of Steel Construction, 2016.
[17] K.D. Tsavdaridis, C. D'Mello, FE investigation of perforated sections with standard and non-standard web opening configurations and sizes, in: S.L. Chan (Ed.), 6th Int. Conf. Adv. is Steel Struct., Hong Kong Institute of Steel Construction, Hong Kong, China, 2009, pp. 213–220.
[18] K.D. Tsavdaridis, Structural Performance of Perforated Steel Beams with Novel Web Openings and with Partial Concrete Encasement, City University London, 2010.
[19] K.D. Tsavdaridis, J.J. Kingman, V.V. Toropov, Application of structural topology optimisation to perforated steel beams, Comput. Struct. 158 (2015) 108–123, http://dx.doi.org/10.1016/j.compstruc.2015.05.004.
[20] F.P.V. Ferreira, R. Shamass, L.F.P. Santos, V. Limbachiya, K.D. Tsavdaridis, EC3 design of web-post buckling resistance for perforated steel beams with elliptically-based web openings, Thin-Walled Struct. 175 (2022) 109196, http://dx.doi.org/10.1016/j.tws.2022.109196.
[21] European committee for standardization, EN 1993-1-1: Eurocode 3 – Design of Steel Structures – Part 1-1: General Rules and Rules for Buildings, 2002.
[22] H.-T. Thai, Machine learning for structural engineering: A state-of-the-art review, Structures 38 (2022) 448–491, http://dx.doi.org/10.1016/j.istruc.2022.02.003.
[23] S. Gholizadeh, A. Pirmoz, R. Attarnejad, Assessment of load carrying capacity of castellated steel beams by neural networks, J. Constr. Steel Res. 67 (2011) 770–779, http://dx.doi.org/10.1016/j.jcsr.2011.01.001.
[24] Y. Sharifi, S. Tohidi, Lateral–torsional buckling capacity assessment of web opening steel girders by artificial neural networks — elastic investigation, Front. Struct. Civ. Eng. 8 (2014) 167–177, http://dx.doi.org/10.1007/s11709-014-0236-z.
[25] S. Tohidi, Y. Sharifi, Inelastic lateral–torsional buckling capacity of corroded web opening steel beams using artificial neural networks, IES J. A Civ. Struct. Eng. 8 (2015) 24–40, http://dx.doi.org/10.1080/19373260.2014.955139.
[26] S. Tohidi, Y. Sharifi, Load-carrying capacity of locally corroded steel plate girder ends using artificial neural network, Thin-Walled Struct. 100 (2016) 48–61, http://dx.doi.org/10.1016/j.tws.2015.12.007.
[27] Y. Sharifi, A. Moghbeli, M. Hosseinpour, H. Sharifi, Neural networks for lateral torsional buckling strength assessment of cellular steel I-beams, Adv. Struct. Eng. 22 (2019) 2192–2202, http://dx.doi.org/10.1177/1369433219836176.
[28] Y. Sharifi, A. Moghbeli, M. Hosseinpour, H. Sharifi, Study of neural network models for the ultimate capacities of cellular steel beams, Iran. J. Sci. Technol. Trans. Civ. Eng. 44 (2020) 579–589, http://dx.doi.org/10.1007/s40996-019-00281-z.
[29] M. Hosseinpour, Y. Sharifi, H. Sharifi, Neural network application for distortional buckling capacity assessment of castellated steel beams, Structures 27 (2020) 1174–1183, http://dx.doi.org/10.1016/j.istruc.2020.07.027.
[30] T.-A. Nguyen, H.-B. Ly, V.Q. Tran, Investigation of ANN architecture for predicting load-carrying capacity of castellated steel beams, Complexity 2021 (2021) 1–14, http://dx.doi.org/10.1155/2021/6697923.
[31] M. Abambres, K. Rajana, K. Tsavdaridis, T. Ribeiro, Neural network-based formula for the buckling load prediction of I-Section cellular steel beams, Computers 8 (2018) 2, http://dx.doi.org/10.3390/computers8010002.
[32] V.V. Degtyarev, K.D. Tsavdaridis, Buckling and ultimate load prediction models for perforated steel beams using machine learning algorithms, J. Build. Eng. 51 (2022) 104316, http://dx.doi.org/10.1016/j.jobe.2022.104316.
[33] K.D. Tsavdaridis, C. D'Mello, Optimisation of novel elliptically-based web opening shapes of perforated steel beams, J. Constr. Steel Res. 76 (2012) 39–53, http://dx.doi.org/10.1016/j.jcsr.2012.03.026.
[34] Dassault Systèmes Simulia, Abaqus 6.18, 2016.

[35] W. Zaarour, R. Redwood, Web buckling in thin webbed castellated beams, J. Struct. Eng. 122 (1996) 860–866, http://dx.doi.org/10.1061/(ASCE)0733-9445(1996)122:8(860).
[36] K.D. Tsavdaridis, G. Galiatsatos, Assessment of cellular beams with transverse stiffeners and closely spaced web openings, Thin-Walled Struct. 94 (2015) 636–650, http://dx.doi.org/10.1016/j.tws.2015.05.005.
[37] S. Durif, A. Bouchaïr, O. Vassart, Experimental and numerical investigation on web-post specimen from cellular beams with sinusoidal openings, Eng. Struct. 59 (2014) 587–598, http://dx.doi.org/10.1016/j.engstruct.2013.11.021.
[38] F.P.V. Ferreira, C.H. Martins, S. De Nardin, Sensitivity analysis of composite cellular beams to constitutive material models and concrete fracture, Int. J. Struct. Stab. Dyn. 21 (2021) 2150008, http://dx.doi.org/10.1142/S0219455421500085.
[39] K. Rajana, K.D. Tsavdaridis, E. Koltsakis, Elastic and inelastic buckling of steel cellular beams under strong-axis bending, Thin-Walled Struct. 156 (2020) 106955, http://dx.doi.org/10.1016/j.tws.2020.106955.
[40] R. Shamass, F. Guarracino, Numerical and analytical analyses of high-strength steel cellular beams: A discerning approach, J. Constr. Steel Res. 166 (2020) 105911, http://dx.doi.org/10.1016/j.jcsr.2019.105911.
[41] F.P.V. Ferreira, K.D. Tsavdaridis, C.H. Martins, S. De Nardin, Ultimate strength prediction of steel–concrete composite cellular beams with PCHCS, Eng. Struct. 236 (2021) 112082, http://dx.doi.org/10.1016/j.engstruct.2021.112082.
[42] F.P.V. Ferreira, C.H. Martins, S. De Nardin, Assessment of web post buckling resistance in steel-concrete composite cellular beams, Thin-Walled Struct. 158 (2021) 106969, http://dx.doi.org/10.1016/j.tws.2020.106969.
[43] F.P.V. Ferreira, K.D. Tsavdaridis, C.H. Martins, S. De Nardin, Buckling and post-buckling analyses of composite cellular beams, Compos. Struct. 262 (2021) http://dx.doi.org/10.1016/j.compstruct.2021.113616.
[44] F.P.V. Ferreira, K.D. Tsavdaridis, C.H. Martins, S. De Nardin, Composite action on web-post buckling shear resistance of composite cellular beams with PCHCS and PCHCSCT, Eng. Struct. 246 (2021) 113065, http://dx.doi.org/10.1016/j.engstruct.2021.113065.
[45] F.P.V. Ferreira, A. Rossi, C.H. Martins, Lateral–torsional buckling of cellular beams according to the possible updating of EC3, J. Constr. Steel Res. 153 (2019) 222–242, http://dx.doi.org/10.1016/j.jcsr.2018.10.011.
[46] MATLAB and Statistics Toolbox Release 2019a, The MathWorks, Inc., Natick, Massachusetts, United States, 2019.
[47] M.J. Moradi, M. Khaleghi, J. Salimi, V. Farhangi, A.M. Ramezanianpour, Predicting the compressive strength of concrete containing metakaolin with different properties using ANN, Measurement 183 (2021) 109790, http://dx.doi.org/10.1016/j.measurement.2021.109790.
[48] J. Jin, M. Li, L. Jin, Data normalization to accelerate training for linear neural net to predict tropical cyclone tracks, Math. Probl. Eng. 2015 (2015) 1–8, http://dx.doi.org/10.1155/2015/931629.
[49] J.D. Olden, D.A. Jackson, Illuminating the black box: a randomization approach for understanding variable contributions in artificial neural networks, Ecol. Model. 154 (2002) 135–150, http://dx.doi.org/10.1016/S0304-3800(02)00064-9.
[50] D.G. Garson, Interpreting neural network connection weights, 1991.
[51] T. Gupta, K.A. Patel, S. Siddique, R.K. Sharma, S. Chaudhary, Prediction of mechanical properties of rubberised concrete exposed to elevated temperature using ANN, Measurement 147 (2019) 106870, http://dx.doi.org/10.1016/j.measurement.2019.106870.
[52] Y. Sharifi, A. Moghbeli, Shear capacity assessment of steel fiber reinforced concrete beams using artificial neural network, Innov. Infrastruct. Solut. 6 (2021) 89, http://dx.doi.org/10.1007/s41062-021-00457-5.
[53] A.M. al Swaidani, W.T. Khwies, Applicability of artificial neural networks to predict mechanical and permeability properties of volcanic scoria-based concrete, Adv. Civ. Eng. 2018 (2018) 1–16, http://dx.doi.org/10.1155/2018/5207962.
[54] J.D. Olden, M.K. Joy, R.G. Death, An accurate comparison of methods for quantifying variable importance in artificial neural networks using simulated data, Ecol. Model. 178 (2004) 389–397, http://dx.doi.org/10.1016/j.ecolmodel.2004.03.013.